ELSEVIER

Thermochimica Acta 398 (2003) 241–248

thermochimica acta

www.elsevier.com/locate/tca

An improved hermetic sample enclosure for simultaneous differential scanning calorimetry/synchrotron powder X-ray diffraction

Dusan Lexa*

Chemical Technology Division, Argonne National Laboratory, 9700 South Cass Avenue, Argonne, IL 60439, USA

Received 29 March 2002; received in revised form 8 July 2002; accepted 9 July 2002

Abstract

A hermetic sample enclosure for performing simultaneous differential scanning calorimetry/synchrotron powder X-ray diffraction, previously developed in our laboratory, suffered from poor calorimetric performance. A new enclosure design has been developed that addresses this problem. Like the previous design, it is based on a Perkin-Elmer DSC-2C measuring head. While the original enclosure necessitated a sample pan rather inconsistent with the requirements of DSC, more sophisticated modifications to the new measuring head made it compatible with a new sample pan that does not compromise calorimetric performance. The original alternative temperature measurement and control system was upgraded with low-noise components. In addition, water-cooling was added to the measuring head. A prototype sample enclosure has been fabricated and successfully tested in multiple experiments.

Keywords: Differential scanning calorimetry; Synchrotron powder X-ray diffraction

1. Introduction

The information content of results obtained from applying two experimental techniques simultaneously is higher than that obtained from an application of the same two techniques separately, as witnessed by the prominence of the so-called "hyphenated techniques" in today's laboratories, e.g., GC-MS, TGA-FTIR. Synchrotron light sources made it possible to devise simultaneous techniques that involve X-rays. Combinations of thermal analysis methods with X-ray methods have become common. Amongst them, simultaneous differential scanning calorimetry and powder X-ray diffraction (DSC/XRD) is one of the most useful.

The advantages of simultaneous DSC/XRD become apparent when one considers the other two approaches to DSC/XRD integration. In sequential DSC/XRD, XRD is performed after a complete DSC scan, or after rapid cool-down at points of interest in the DSC scan. This only gives a structural snapshot of the sample at a given moment of sample history. There is also the possibility of sample transformation due to finite cool-down rates. In parallel DSC/XRD, the DSC and XRD are performed on different samples. Hence, correlation of thermal and structural information can be ambiguous as a result of sampling, i.e., the DSC and the XRD samples might not be exactly the same material. None of the above problems is encountered in simultaneous DSC/XRD. However, the design of a simultaneous DSC/XRD system can be challenging. (Simultaneous DSC/XRD will hereafter

* Tel.: +1-630-252-6747; fax: +1-630-252-9917.
E-mail address: lexa@cmt.anl.gov (D. Lexa).

0040-6031/03/$ – see front matter © 2002 Published by Elsevier Science B.V.
PII: S0040-6031(02)00389-1

be referred to simply as “DSC/XRD”.) Designing a DSC/XRD system can be done either ab initio [1] or by modifying a commercially available DSC instrument for simultaneous XRD operation. Because of the high level of sophistication of today’s DSC instruments, the latter route has almost exclusively been followed. Of the two types of DSC instruments, heat-flux and power-compensation, most DSC/XRD systems have been based on the former [2–6]. However, because of a furnace surrounding the sample and reference cells, heat-flux DSC modifications involve either creating an X-ray path through the furnace for horizontal operation [6] (reflection geometry) or using various inserts to keep the sample and reference pans in place for vertical operation [2–5] (transmission geometry). Both approaches compromise DSC performance. These difficulties can be overcome by using a power-compensated DSC instrument [7–9]. Hence, this approach was chosen for the development of a DSC/XRD system in this laboratory.

The original, hereafter referred to as “old-design”, hermetic enclosure for DSC/XRD has been described previously [10]. The results of experiments performed with the old-design DSC/XRD system have been published elsewhere [11]. The improved hermetic enclosure for DSC/XRD, hereafter referred to as “new-design”, has been developed to address the problems encountered with the old-design system.

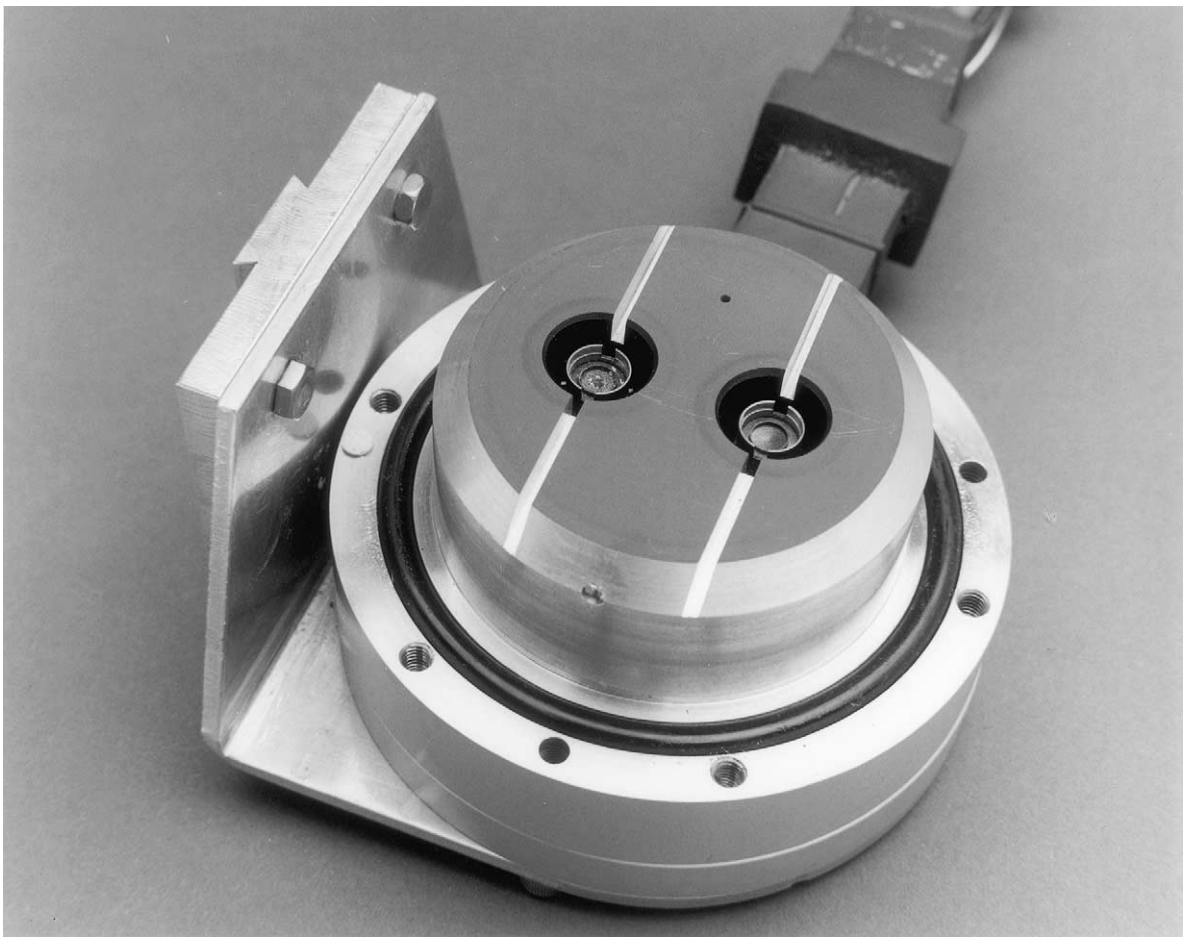

Fig. 1. Photograph of the open DSC/XRD measuring head. The Pt sample (left) and reference (right) cups are occupied by empty graphite pans. Remnants of a sample are visible on the graphite pan and the sample itself can be seen on the support bracket.

It was designed for and tested on a Huber 8-circle diffractometer at the Materials Research Collaborative Access Team (MR-CAT) beam line of the Advanced Photon Source (APS) at Argonne National Laboratory (ANL).

2. Design

The new-design hermetic enclosure is shown in Figs. 1 and 2. The engineering details are shown in Fig. 3. In the old-design, a layer of material from the top of the head base was removed so that the tops of the Pt cups were flush with the new top surface of the head base. The graphite sample pan with a height of 3.5 mm (0.138 in.)—identical to the Pt sample cup depth—required a cylindrical sample 5.0 mm (0.197 in.) in diameter and 3.0 mm (0.118 in.) thick to make the sample surface flush with the top of the Pt sample cup (and the surface of the head base) and, thus, accessible to X-rays. The extreme thickness of the sample (by DSC standards) resulted in a decrease in DSC resolution and an increase in the vertical thermal gradient in the sample, which compromised the very essence of the method: the accurate correlation of DSC and XRD data. While both of these effects might be partially mitigated by decreasing the scanning rate to 10 K min^{-1} or lower, for example, decreasing the

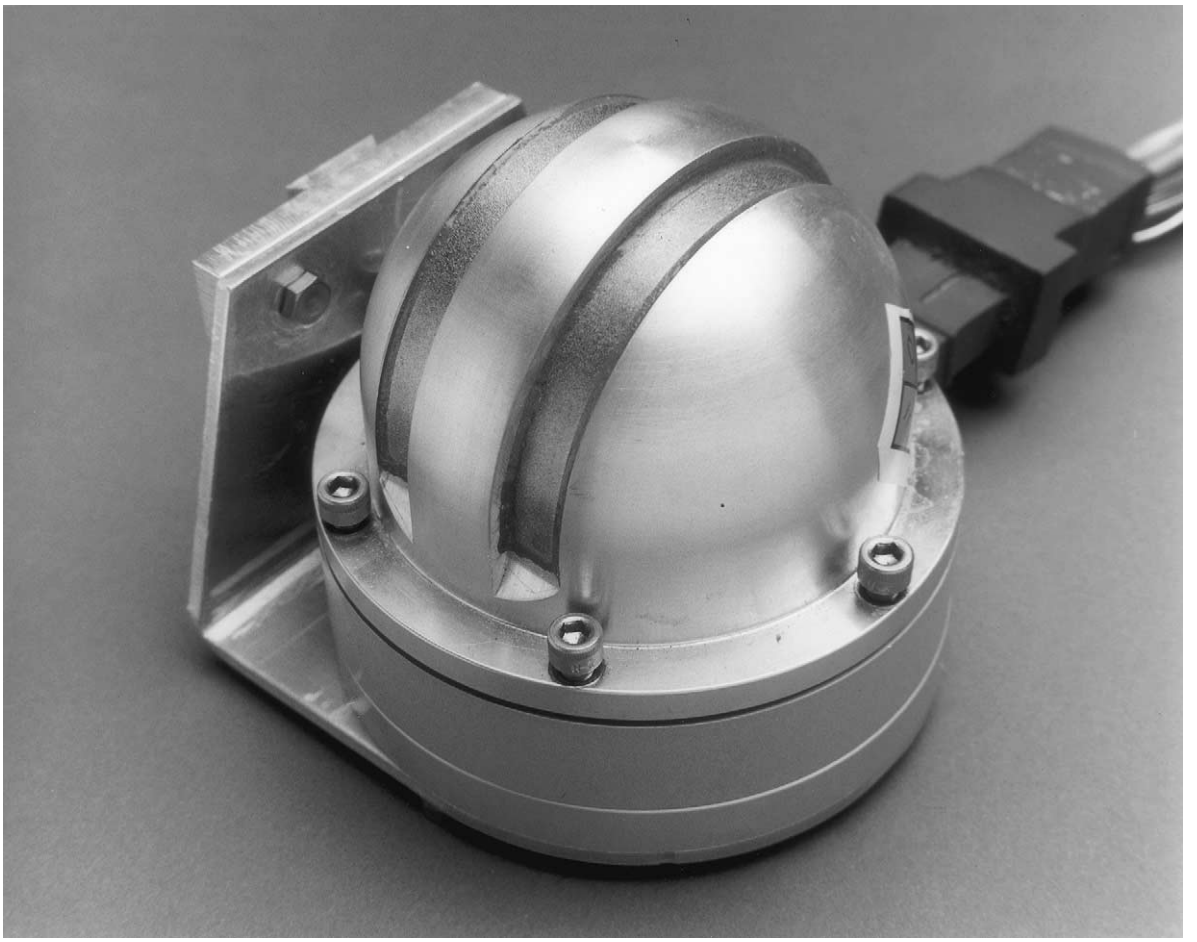

Fig. 2. Photograph of the closed DSC/XRD measuring head. The beryllium windows and their epoxy seals can be seen as well as the heat exchanger body between the head base and the support bracket.

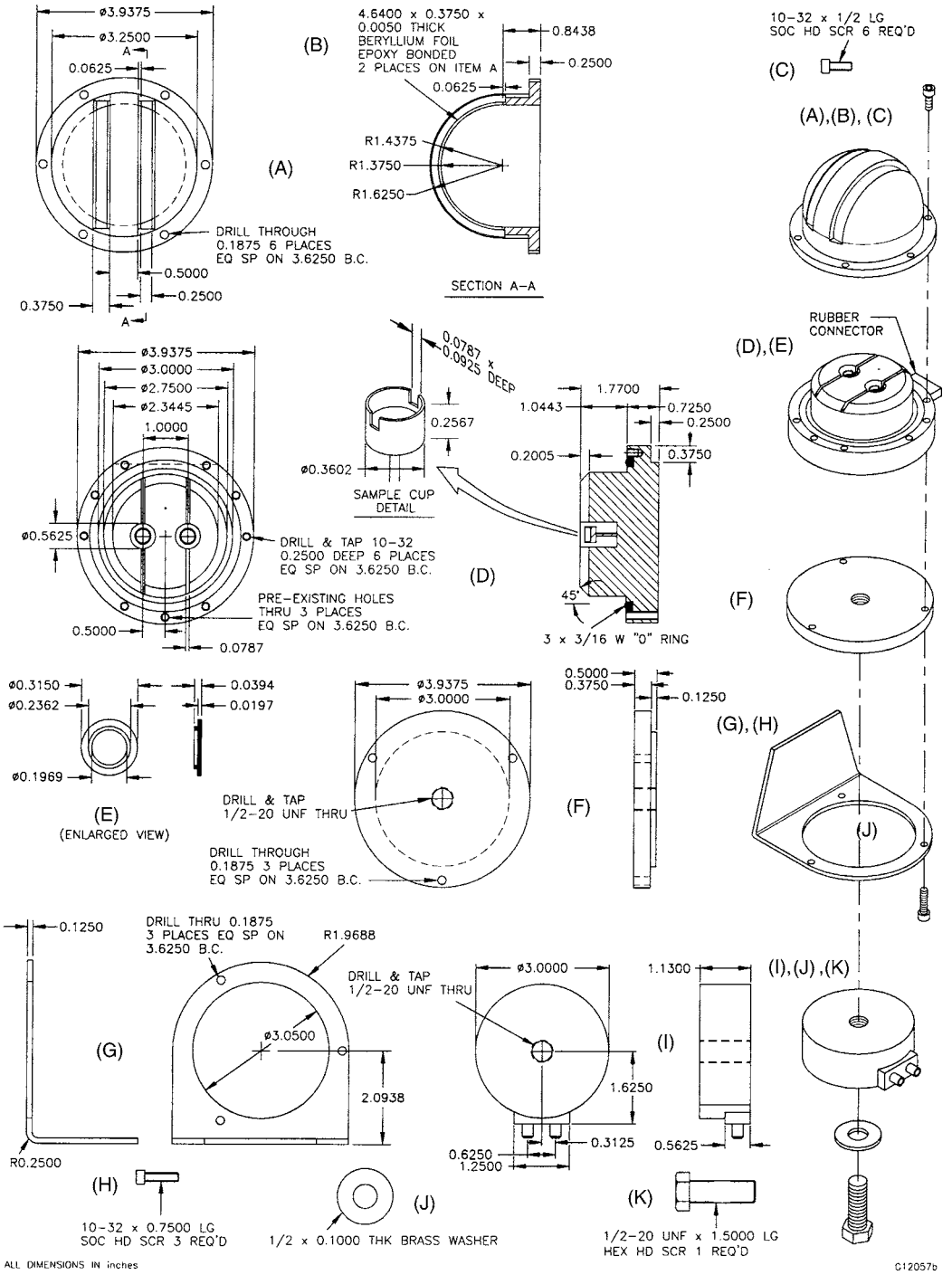

Fig. 3. Assembly drawing and sectional views of the DSC/XRD measuring head components.

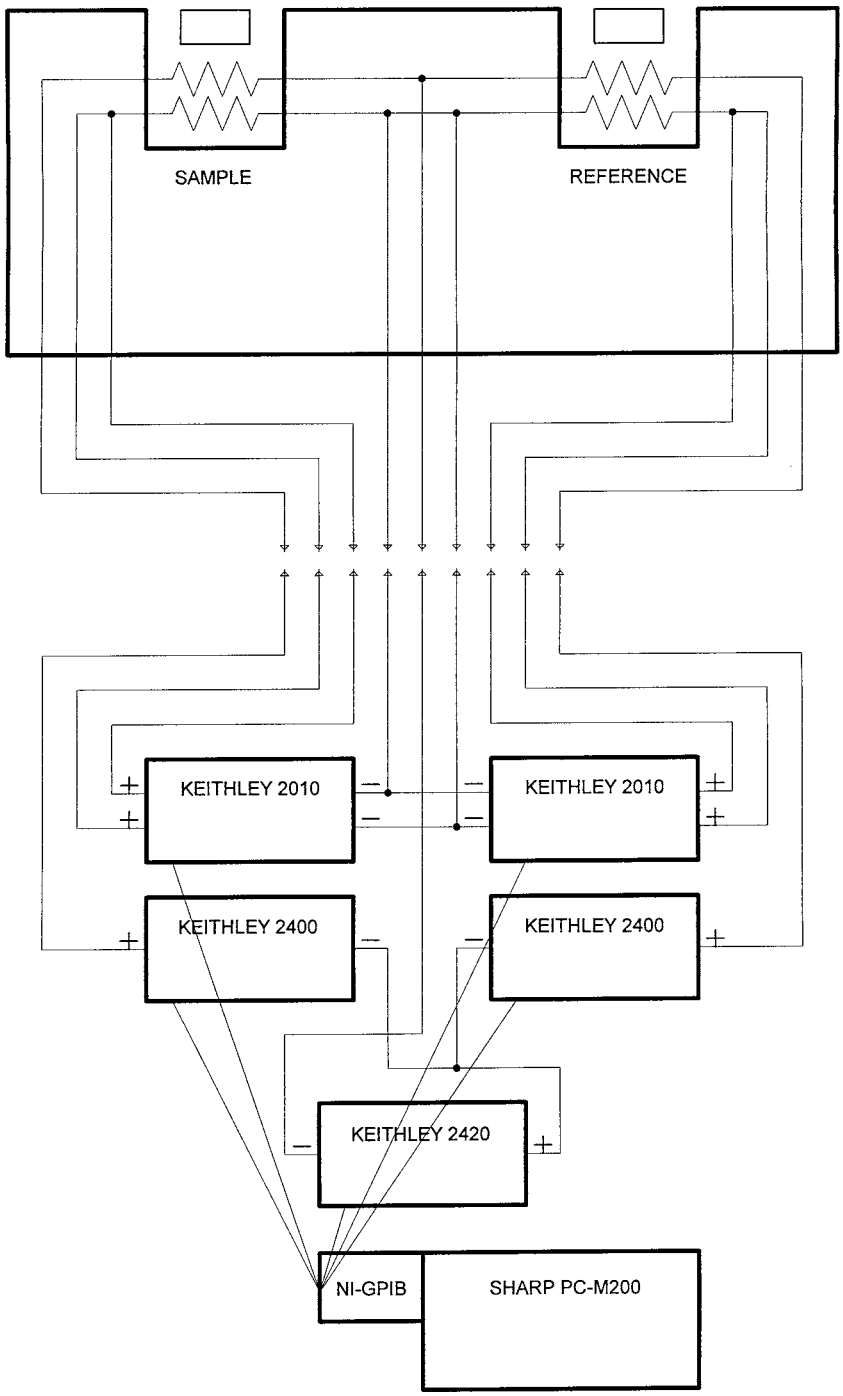

Fig. 4. Electrical diagram of the DSC/XRD measuring head and the ATMCS.

sample thickness to an acceptable level is clearly the most effective solution and was, therefore, pursued. While the diameter of the sample pan base remained unchanged at 8.0 mm (0.315 in.) to ensure a tight fit inside the Pt sample cup, the height of the sample pan was decreased from 3.5 mm (0.138 in.) to 1.0 mm (0.039 in.), see Fig. 3(E). A cylindrical sample 5.0 mm (0.0.197 in.) in diameter and only 0.5 mm (0.020 in.) thick is now required—well within the optimal DSC sample thickness range of up to 1 mm (0.039 in.). The sample surface is now 2.35 mm (0.093 in.) below the edge of the 3.35 mm (0.132 in.) deep Pt sample cup. In order to allow the X-ray beam unobstructed access to the sample, the Pt sample (and, for reasons of DSC symmetry, the reference) cup had to be modified. Following removal of the Pt sample and reference cups from the head base, two diametrically opposite notches, 2.00 mm (0.079 in.) wide and 2.35 mm (0.093 in.) deep, were then cut into the upper edge of each cup by wire electrical discharge machining, see Fig. 3(D). With the cups removed from the head base, two parallel channels, 2.00 mm (0.079 in.) wide and 5.15 mm (0.203 in.) deep, were machined into its top surface, see Fig. 3(D). The top edge of the head base was machined into a 45° taper to accommodate the old-design head cover, which is now positioned 2.35 mm (0.093 in.) lower than on the old-design head base. The Pt sample and reference cups were then re-inserted into the head base so that the notches in the cups and the channels in the head base were aligned. In order to improve high-temperature operation characteristics, water-cooling was provided, consisting of a modified DSC-2C water-cooling system, see Fig. 3(F, I, J, K).

The previously developed alternative temperature measurement and control system (ATMCS) [10], emulating the functions of a DSC-2C type instrument [12], generated exceedingly high noise levels in the DSC signal. The problem was traced to insufficient temperature measurement, voltage-programming, and voltage-measurement resolution, computer system clock inaccuracy, and the ATMCS software. The schematic of a new ATMCS addressing these problems is shown in Fig. 4. Temperature measurement is performed by two Keithley 2010 low-noise digital multimeters (resolution of 10 μΩ on a 100 Ω range, corresponding to a temperature resolution of 2.2 mK) connected to the Pt resistance thermometers via a 4-probe scheme. Differential electrical power is delivered to the resistance heaters by two Keithley 2400 SourceMeter® instruments (voltage-programming resolution of 50 μV on a 2 V range, voltage-measurement resolution of 10 μV on a 2 V range, current-measurement resolution of 10 μA on a 1 A range). Common electrical power is provided by a Keithley 2420 high-current SourceMeter®. All five instruments are controlled remotely from a Sharp PC-M200 notebook computer running Windows 95 via a National Instruments PCMCIA-GPIB interface. The ATMCS software, written in MS Visual Basic 5.0, performs the function of a dual PID controller [13,14]. The computer system clock is no longer accessed by the software. Temperature readings and power adjustments are made with a frequency of 2.5 Hz. Both sample and reference are kept at a constant or linearly rising temperature. The difference between power (calculated as a product of the voltage and current measured by each of the two Keithley 2400 SourceMeter® instruments) applied to the sample and reference Pt resistance heaters, respectively, is the DSC signal.

3. Performance

Multiple experiments have been performed with the new-design DSC/XRD system at the MR-CAT beam line of the APS at ANL. The open head with a sample pan containing zinc sulfide (a fluorescent substance) has been attached to an *X–Y* stage in the center of the Huber 8-circle diffractometer, inclined at an angle θ of 3° relative to the horizontal, and precisely aligned by remote observation of the fluorescing spot and manipulation of the *X–Y* stage. The head has then been removed from the *X–Y* stage, charged with a pan containing the sample in place of the zinc sulfide, sealed hermetically with the head cover, and reattached to the *X–Y* stage. Gas, cooling-water, and electronics connections have been made, followed by fine alignment using XRD on the sample. Mixtures of the LiCl–KCl eutectic salt and dehydrated zeolite have been studied by simultaneous DSC/XRD at a heating rate of 10 K min^{-1} between 300 and 800 K. The wavelength of the synchrotron radiation, λ was 1.127 A, and XRD patterns between 2θ of 4° and 45° were collected every 10 K at a scanning rate of 1° s^{-1}.

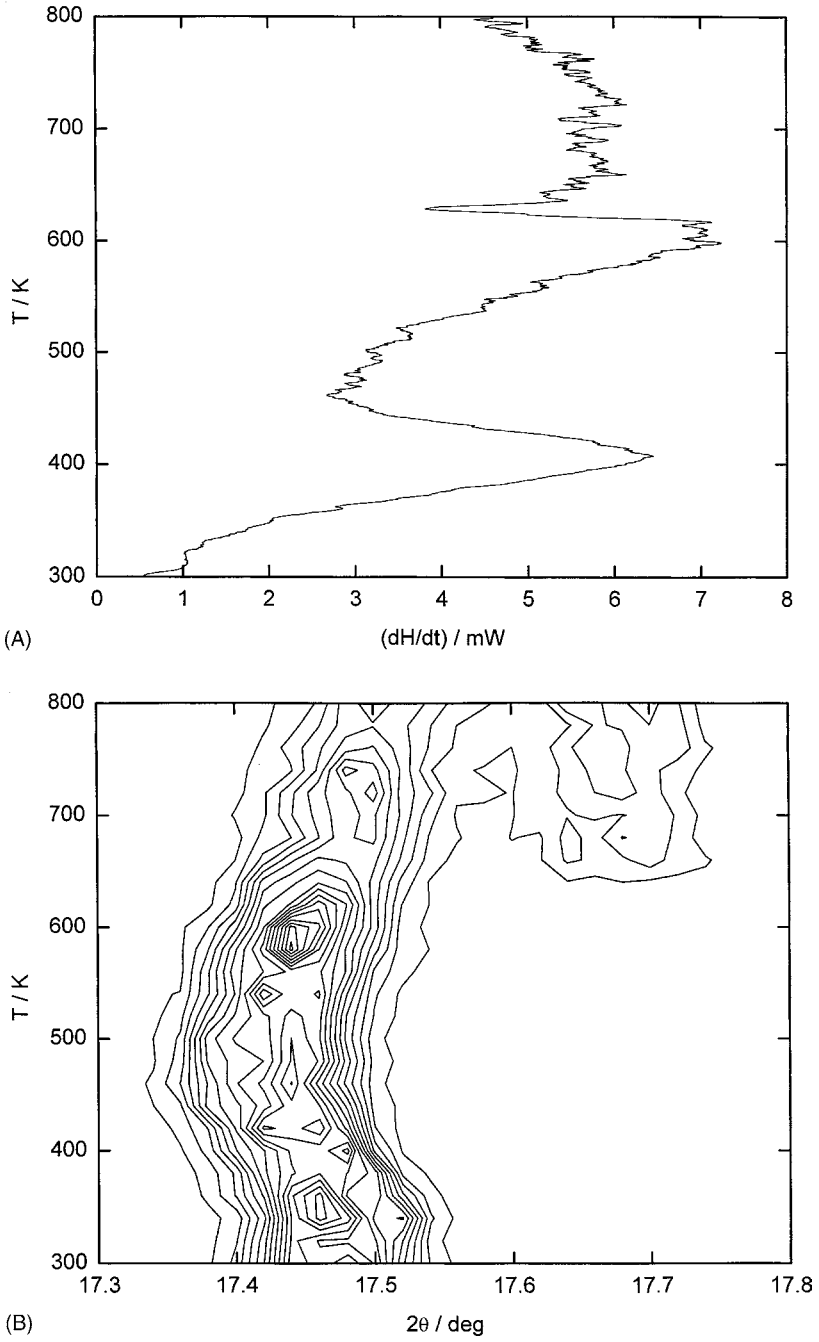

Fig. 5. (A) Results of a DSC scan on a mixture of the LiCl–KCl eutectic salt and zeolite. Heating rate 10 K min^{-1}. Zeolite dehydration endotherm at ~400 K; salt melting and occlusion exotherm at ~630 K. (B) Results of an XRD scan on a mixture of the LiCl–KCl eutectic salt and zeolite. Scanning rate 1° s^{-1}. Zeolite diffraction peak at ~17.45°; thermal expansion between 300 and 500 K; salt occlusion between 500 and 800 K. New zeolite diffraction peak appearance at ~17.65° and ~630 K.

The DSC plot resulting from one of the experiments is shown in Fig. 5(A), and the associated XRD plot is shown in Fig. 5(B). It is seen, for example, that the appearance of a zeolite diffraction peak at ∼17.65° and ∼630 K in the XRD plot exactly coincides with the exotherm at ∼630 K in the DSC plot. Full results of these experiments will be published elsewhere.

The old-design ATMCS exhibited a 10 K min^{-1} scanning peak-to-peak noise of ∼2.5 mW at 450 K. A more detailed study of the new-design ATMCS behavior showed that the isothermal root-mean-square noise changes approximately linearly from 0.05 mW at 300 K to 0.30 mW at 800 K, a significant improvement. However, Perkin-Elmer product literature indicates a temperature-independent (probably room temperature) isothermal root-mean-square noise level of 0.005 mW for DSC-2C, 0.004 mW for DSC 4, 0.5 μW for DSC 7, and 0.1 μW for the current Pyris 1 DSC. Hence, it is clear that, while indispensable in the proof-of-concept phase of this work, even the new-design ATMCS is inferior to the commercial units. The difference, however, may not be as dramatic as the numbers suggest. This is because no smoothing was performed by the ATMCS software, while the commercial units are known to use sophisticated smoothing algorithms. Nevertheless, work has already been completed on the integration of the Perkin-Elmer Pyris 1 DSC unit into a state-of-the-art DSC/XRD system [15].

Acknowledgements

The author would like to thank Mr. W.G. Brown and his staff for fabricating the hermetic enclosure prototype, and Mr. T.J. Lucitt for producing the engineering drawings.

Use of the Advanced Photon Source was supported by the US Department of Energy, Basic Energy Sciences, Office of Energy Research (DOE-BES-OER), under contract no. W-31-109-Eng-38. The MR-CAT beam lines are supported by the member institutions and the US DOE-BES-OER under contracts DE-FG02-94ER45525 and DE-FG02-96ER45589.

References

[1] G. Keller, F. Lavigne, L. Forte, K. Andrieux, M. Dahim, C. Loisel, M. Ollivon, C. Bourgaux, P. Lesieur, J. Therm. Anal. 51 (1998) 783.
[2] G. Ungar, J.L. Feijoo, Mol. Cryst. Liq. Cryst. 180B (1990) 281.
[3] H. Chung, M. Caffrey, Biophys. J. 63 (1992) 438.
[4] W. Bras, G.E. Derbyshire, A. Devine, S.M. Clark, J. Cooke, B.E. Komanschek, A.J. Ryan, J. Appl. Crystallogr. 28 (1995) 26.
[5] H. Yoshida, R. Kinoshita, Y. Teramoto, Thermochim. Acta 264 (1995) 173.
[6] A. Kishi, T. Arii, Y. Kobayashi, Y. Yamada, M. Nakayama, S. Munekawa, in: Proceedings of the 48th Annual Denver X-ray Conference, Steamboat Springs, CO, 1999.
[7] T.G. Fawcett, C.E. Crowder, L.F. Whiting, J.C. Tou, W.F. Scott, R.A. Newman, W.C. Harris, F.J. Knoll, V.J. Caldecourt, Adv. X-ray Anal. 28 (1985) 227.
[8] T.G. Fawcett, W.C. Harris Jr., A. Newman, L.F. Whiting, F.J. Knoll, US Patent 4 821 303 (April 11, 1989).
[9] T. Arii, A. Kishi, Y. Kobayashi, Thermochim. Acta 325 (1999) 151.
[10] D. Lexa, Rev. Sci. Instrum. 70 (1999) 2242.
[11] D. Lexa, L. Leibowitz, A.J. Kropf, J. Nucl. Mater. 279 (2000) 57.
[12] E.S. Watson, M.J. O'Neill, J. Justin, N. Brenner, Anal. Chem. 36 (1964) 1233.
[13] M.J. O'Neill, Anal. Chem. 36 (1964) 1241.
[14] S. Tanaka, Thermochim. Acta 210 (1992) 67.
[15] D. Lexa, Thermochim. Acta, submitted for publication.